

## A Converter Efficiency, Optimization Method Under Light-Load

P. Vijayan and R.Sridevi

<sup>1</sup>P.G.<sup>2</sup>Assistant Professor,

<sup>1,2</sup>EEE Department, SKP Engineering College, Tiruvannamalai

<sup>1</sup>vijayan.pandu@gmail.com, <sup>2</sup>srisuhar06@gmail.com

**Abstract**—In this paper, a method of maintaining high powerconversion efficiency across the entire load range and its circuit implementations are described. The proposed method substantially increases the conversion efficiency at light loads by minimizing switching and driving losses of semiconductor switches, as well as core losses of magnetic components. These losses are minimized by periodically turning off and on the power converter, and by controlling the converter so that when the converter is ON, it operates at the power level that exhibits the maximum efficiency. The performance of the proposed method was evaluated on a 500-W, 400-V/12-V dc-dc converter and a 1-kW ac-dc boost power-factor correction front-end.

**Index Terms**—Efficiency optimization, light load, maximum efficiency, power management.

### I. INTRODUCTION

EVER since the start of the miniaturization era spurred on by the microelectronics revolution of the late 1950s and early 1960s, power-conversion equipment has been facing continuously increasing power density and efficiency challenges. Until recently, efficiency increases of power conversion circuits were primarily driven by increased power density requirements, since power density increases are possible only if appropriate incremental improvements in full-load efficiency are achieved, so that the thermal performance is not adversely affected. As a result, maximization of the full-load efficiency has been a design focus all along. However, in the late 1990s, the explosive growth of consumer electronics and data-processing equipment has prompted the introduction of various, mostly voluntary, requirements aimed at minimizing the idle-mode, i.e., light-load, power consumption. Meeting these increasingly stringent requirements, most notably those defined in the U.S. Energy Star, Japan Top Runner, and European Code of Conduct (EcoC) specifications [1], still poses a major design challenge. Today, the power supply industry is at the beginning of another major focus shift that puts efficiency improvements across the entire load range in the forefront of customers' performance requirements. This focus on efficiency has been prompted by economic reasons and environmental concerns caused by the continuous aggressive growth of the Internet infrastructure and a relatively low energy

efficiency of its power delivery system. In fact, the environmental concerns have already prompted introduction of programs and initiatives aimed at reducing the energy waste in power supplies for data-processing applications by challenging power-supply manufacturers to improve efficiencies of their products. For example, the 80 Plus incentive program [2] and Climate Saver Computing Initiative (CSCI) [3], [4], the two programs that are already in place, require that power supplies for computer applications maintain efficiency above 80% in the entire load range, from full load down to 20% of full load. These efficiency targets have recently been incorporated into the latest U.S. Environmental Protection Agency's (EPA) Energy Star specifications [5]. However, many of the largest computer, telecom, and network equipment manufacturers already require light-load efficiencies that exceed the latest Energy Star specifications and are also extending these requirements down to 10% and even 5% loads. Generally, the efficiency of power-conversion circuits at heavy loads is determined by the conduction losses of semiconductor and magnetic components, whereas their light-load efficiency is primarily determined by switching losses of semiconductors, core losses of magnetics, and drive losses of semiconductor switches. Because switching and drive losses of semiconductor switches and core losses of magnetic components are almost independent of the load, a typical efficiency curve as a function of the load power shows a steep falloff as the load decreases below 10%–20% of the full load, as illustrated in Fig. 1. Furthermore, as the rated output power of the converter increases, larger semiconductor devices (or more devices in parallel) and larger magnetic cores are needed, which leads to increased switching and core losses, and an even steeper falloff of efficiency at light loads. To make the power supply exhibit a flatter efficiency curve that meets customers' expectations, power management techniques, such as variable switching frequency control, bulk voltage reduction, phase-shedding, and "burst"-mode operation, have been introduced [8]–[11].

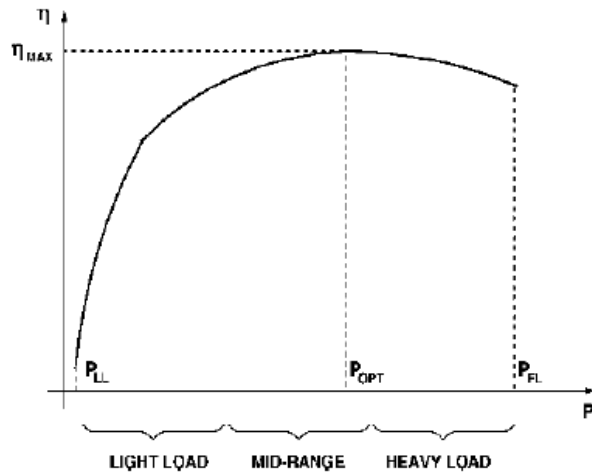


Fig. 1. Typical efficiency profile of a power converter with respect to the power delivered.

Although the described techniques have been shown to improve the partial load efficiency, they suffer from some major drawbacks that limit their area of application. For example, a major problem of reducing the switching frequency at light loads is an increased current ripple caused by the increased volt-second product in the core of the output filter inductor. This increase in the ripple current has an adverse effect on the efficiency because it increases the conduction loss. A major concern with bulk voltage reduction and stage-shedding techniques is the dynamic performance, specifically their ability to restore full-power capability without output disturbance or other performance deterioration when the load suddenly changes from light load to full load. Finally, “burst”- mode operation is limited to very low power levels primarily due to acoustic noise.

In this paper, a method of maintaining high power-conversion efficiency across the entire load range and its circuit implementations are described. Specifically, the proposed method substantially increases the conversion efficiency at light load by minimizing switching and driving losses of semiconductor switches, as well as core losses of magnetic components. These losses are minimized by periodically turning off and on the power converter with a duty cycle set so that when the converter is ON, it operates at the power level that exhibits the maximum efficiency. The required output power during the periods when the converter is turned off is supplied from an energy-storage device. The operation and light-load efficiency performance of the proposed method was verified on a 500-W, 400-V/12-V dc/dc converter, and a 1-kW ac/dc boost power-factor-correction (PFC) front-end.

## II. METHOD DESCRIPTION

The proposed method of light-load efficiency optimization is based on a simple observation that the minimization of power loss requires that the power converter is either always operated at the load power with the maximum efficiency or be completely turned off, i.e., by restricting the operation of a converter to only these two operating points, the best possible efficiency can be achieved because when the converter is turned off, no loss is incurred, whereas when the converter is turned on, it operates with the maximum efficiency. A conceptual block diagram of the proposed light-load efficiency optimization method is shown in Fig. 2. The temporary energy storage and power conditioning block in Fig. 2 serves to maintain a continuous supply of load power during the periods the power converter is turned off. At power levels during which the power converter is continuously ON, this temporary energy storage and power conditioning block is idle, since the entire required load power is supplied by the power converter

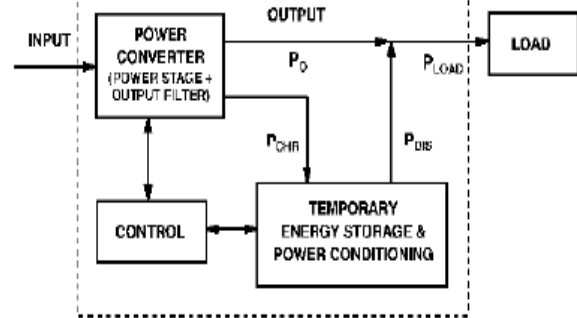


Fig. 2. Conceptual block diagram of the proposed light-load efficiency optimization method.

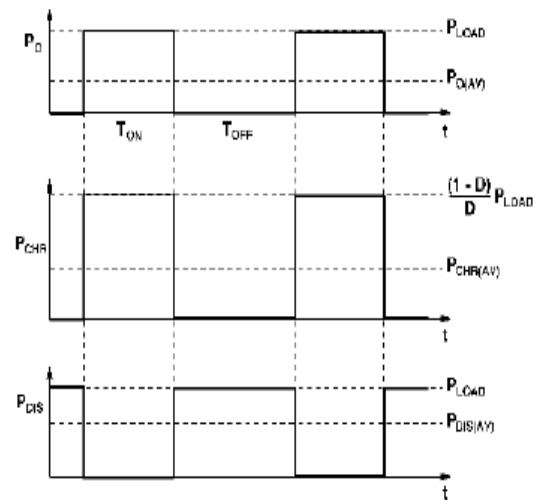
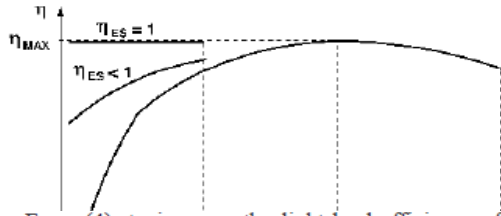


Fig. 3. Timing diagram of output power  $P_O$ , charging power  $P_{CHR}$ , and discharging power  $P_{DIS}$ .



From (4), to improve the light-load efficiency of a power converter with the efficiency dependence on delivered power as in Fig. 1, optimal duty cycle  $D_{OPT}$  should be selected from (4) as

$$D_{OPT} = \frac{P_{LOAD}}{P_{OPT}} \quad (5)$$

i.e., the power converter during  $T_{ON}$  should deliver power  $P_{OPT}$  that corresponds to the maximum efficiency.

Theoretically, the power level that this method of efficiency optimization can be applied is limited to the power level below  $P_{OPT}$ . Typically, the boundary load power between continuous and pulse modes of operation of the power converter  $P_{BOUND}$  ( $< P_{OPT}$ ) is set at light-load levels where efficiency falloff becomes pronounced, as illustrated in Fig. 4.

In the derivation of  $D_{OPT}$  in (5), it was assumed that no loss is incurred during the charging and discharging of the energy-storage device. If charging and discharging losses are included by assuming that the energy-storage device charging and discharging efficiencies are  $\eta_{CHR}$  and  $\eta_{DIS}$ , respectively, then the optimal duty cycle  $D_{OPT}^*$  is

$$D_{OPT}^* = \frac{1}{(P_{OPT}/P_{LOAD})\eta_{ES} + (1 - \eta_{ES})} \quad (6)$$

where  $\eta_{ES} = \eta_{CHR}\eta_{DIS}$  is the efficiency of the energy storage and power conditioning block.

entirely supported by the discharging of the energy-storage device, i.e.,  $P_{DIS} = P_{LOAD}$ . According to Fig. 3, average power  $P_{O(AV)}$  delivered by the power converter to the load is

$$P_{O(AV)} = DP_{LOAD} \quad (1)$$

and average power  $P_{DIS(AV)}$  delivered by the energy-storage device to the load is

$$P_{DIS(AV)} = (1 - D)P_{LOAD} \quad (2)$$

where  $D = T_{ON}/(T_{ON} + T_{OFF})$ .

Since average charging power  $P_{CHR(AV)}$  must be equal to average discharging power  $P_{DIS(AV)}$ , the instantaneous charging power  $P_{CHR}$  during  $T_{ON}$  is

$$P_{CHR} = \frac{(1 - D)}{D}P_{LOAD} \quad (3)$$

as illustrated in Fig. 3.

Therefore, total instantaneous power  $P$  delivered by the power converter during  $T_{ON}$  is

$$P = P_O + P_{CHR} = P_{LOAD} + \frac{1 - D}{D}P_{LOAD} = \frac{P_{LOAD}}{D} \quad (4)$$

where  $\eta_{ES} = \eta_{CHR}\eta_{DIS}$  is the efficiency of the energy storage and power conditioning block. With charging and discharging losses included, the conversion efficiency at power levels below  $P_{BOUND}$  is given by  $\eta_{ES}$

Many variations of the proposed efficiency optimization method are possible. Generally, these variations are related to realization of the charging and discharging

paths of the energystorage device. For example, the charging energy can be supplied from the input of the power converter instead of from the output.

$$\eta = \eta_{MAX - OPT}(1 - \eta_{ES})$$

(7) Also, the proposed method can be implemented with a common charging and discharging path. Furthermore, the charging and In the ideal case, when no energy is lost during the charging and discharging of the energy-storage device, i.e., when it is assumed that  $\eta_{ES} = 1$ , light-load efficiency is equal to  $\eta_{MAX}$  all the way to a minimum load, as illustrated in Fig. 4. However, in practice, because  $\eta_{ES} < 1$ , the light-load efficiency is less than  $\eta_{MAX}$ , and exhibits a falloff as power is reduced, as shown in Fig. 4. Generally, to achieve light-load efficiency improvement,

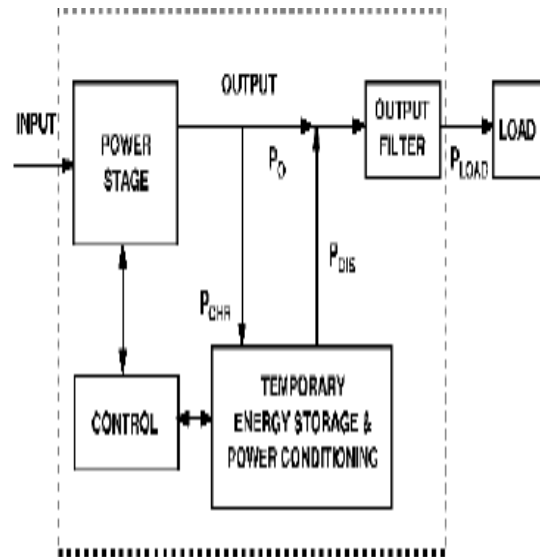


Fig. 5. Conceptual block diagram of another implementation of the proposed light-load efficiency optimization method.

periodic turning on and off of the power converter. Namely, since in these implementations, the output filter inductor current is continuously flowing, i.e., it is either supplied from the converter or from the discharging energy-storage device, it does not exhibit significant transients if the circuit is designed so that the current supplied by the converter when it is ON and the current supplied by the energy-storage and conditioning circuit during the OFF-time are reasonably matched.

### III. CIRCUIT IMPLEMENTATIONS

Figs. 6(a)–(e) shows several dc–dc converter implementations of the proposed efficiency optimization method. The power stage box in the figures can be any single or interleaved powerconversion topology, such as half-bridge, full-bridge, single or two-switch forward, or *LLC* topology. Fig. 6(a)–(c) shows the implementations of the concept according to Fig. 5 where the discharging path of the energy-storage devices, i.e., capacitor  $C_{ST}$ , is through the output filter of the power converter. Fig. 6(d) and (e) shows examples of circuit implementations of the proposed method according to Fig. 2, where the charging and discharging paths of energy-storage cap  $C_{ST}$  are coupled directly to the output.

In the implementation in Fig. 6(a), energy-storage capacitor  $C_{ST}$  is inductively charged by a dc output of the power stage when the power stage is turned on. During the time periods the power stage is turned off, the load power  $I_s$  is provided by discharging  $C_{ST}$  through a buck converter that shares the output filter with the power stage. Generally, for isolated power converter stages, inductance  $L_1$  in the charging path can be the leakage inductance of the transformer. The implementation of  $L_1$  as the leakage inductance of the transformer is especially effective in topologies where the leakage inductance of the transformer is intentionally increased, such as in the full-bridge converter with phase-shift control or *LLC* resonant converter.

The implementation in Fig. 6(b) employs a boost converter to charge energy-storage capacitor  $C_{ST}$  and a buck converter in the discharging path. Because of the boost converter, energy storage in capacitor  $C_{ST}$  can be done at a higher voltage, which makes it possible to reduce the size of the energy-storage capacitor. A variation of this implementation that employs a common charging and discharging path is shown in Fig. 6(c). In this implementation, a bidirectional buck–boost converter is used to provide controlled charging and discharging of the energystorage capacitor. Fig. 6(d) shows an implementation where the charging and discharging paths of capacitor  $C_{ST}$  are coupled to the output of the power converter. In fact, this implementation is a variation of the implementation in Fig. 6(c) since the boost converter is used for charging and the buck for discharging.

Finally, Fig. 6(e) shows the simplest implementation of the proposed method. In this implementation, energy-storage capacitor  $C_{ST}$  is directly connected in parallel with output filter capacitor  $C_F$ . In fact, in applications where the output filter Fig. 7. Control implementation of the proposed method in PFC applications. capacitor needs to store significant energy, for example, in PFC applications, additional energy-storage capacitor  $C_{ST}$  may not be needed.

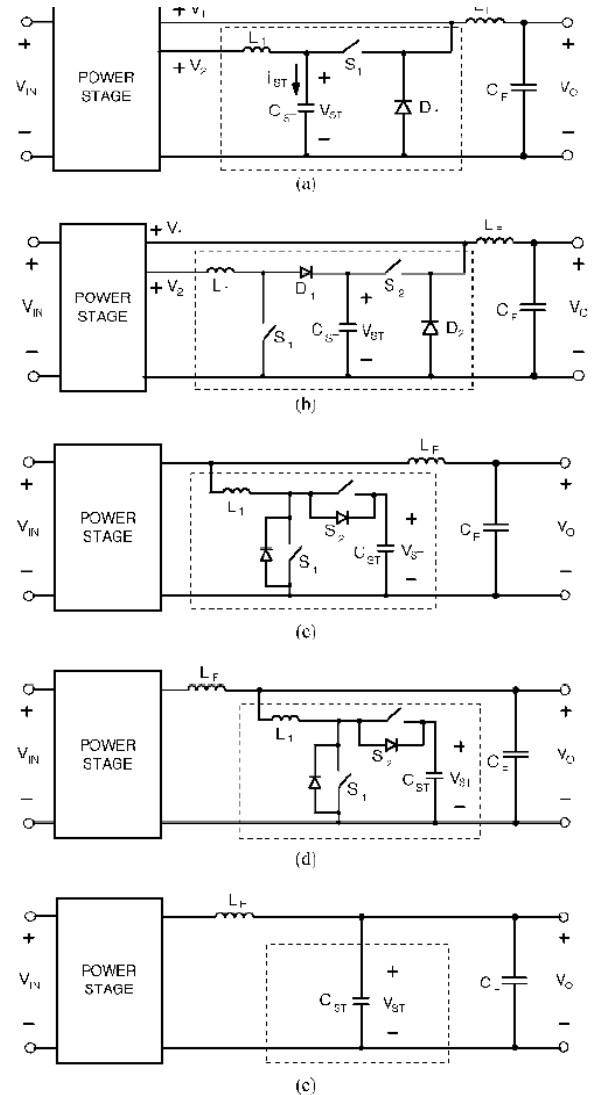


Fig. 6. Examples of circuit implementations of the proposed light-load efficiency optimization method.

When the proposed efficiency optimization method is applied to the ac–dc PFC front-end, it is necessary to recognize that the line current harmonic limit specifications need to be met down to 75 W of input power [12]. As a result, a straightforward implementation of this method, where the front-end power converter is periodically turned on and off with an arbitrary frequency, is possible only below the input power of 75 W. Because of the required compliance with the line current harmonic limit specifications at input power levels above 75 W, the turning off and on of the converter can only be done within half-line cycles, as illustrated in Fig. 7. In the control approach shown in Fig. 7, the PFC converter is kept OFF near the zero crossings of the line current, and is enabled for power processing around the peaks of the line current. Since this conduction-angle control generates line current distortions that increase as turn-

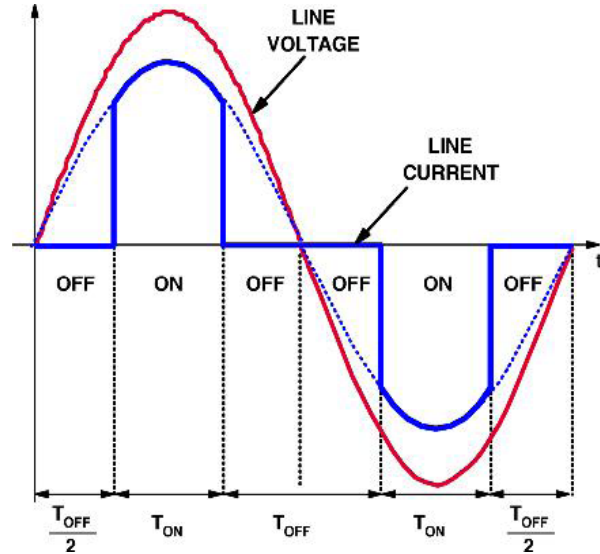
OFF time  $T_{OFF}$  increases, the maximum duration of OFF-time  $T_{OFF}$  is limited by the required harmonic-limit compliance of the line current. This maximum OFF-time can be easily figured out for a given power level either by using simulation or calculation software.

#### IV. EXPERIMENTAL RESULTS

The performance of the proposed technique was separately evaluated on a 500-W dc–dc converter and a 1-kW ac–dc PFC boost frontend rectifier. The circuit diagram of the 500-W dc–dc converter prototype is shown in Fig. 8. The circuit in Fig. 8 implements the proposed method of light-load efficiency optimization according to Fig. 6(a), where  $V1 = V2$  and  $L1$  is the leakage inductance of transformer TR, i.e., it combines a zero-voltage-switching (ZVS) full-bridge converter with phase-shift control with a synchronous buck converter discharging circuit. The 500-W dc–dc prototype was designed to operate from a 400-V dc input and deliver up to 42 A at a 12-V output. Fig. 8. Circuit diagram of 500-W, ZVS full-bridge dc–dc converter laboratory prototype. Added temporary energy storage and power conditioning circuit are shown inside the dashed-line rectangle.

The full-bridge converter operating at 110-kHz switching frequency was implemented with an IRFP23N50L MOSFET from IR for each bridge switch Q1–Q4, whereas a FDB045AN08 MOSFET from Fairchild was employed for each synchronous rectifier SR1 and SR2. Transformer TR was built using a pair of ferrite E-cores (E34/26/9-H7C4) with 44 turns of magnet wire (AWG #18) for the primary winding and 2 turns of copper foil (10 mil, 20 mm) for each of the secondary windings. Output filter inductor LF was built using a toroidal high-flux core (58894A2,  $\mu = 60$ ) from Magnetics with eight turns of magnet wire (six strands, AWG #18). Four low-voltage aluminum capacitors (1000  $\mu$ F, 16 Vdc) were used for output capacitor CF. The buck converter that is periodically turned on at light loads to deliver power from energy-storage capacitor CST was implemented with an FDP047AN08 MOSFET from Fairchild for both the buck switch S1 and synchronous rectifier switch S2. Schottky diodes MBR1080G from On Semi were used for charging diodes D1 and D2. Finally, six low-voltage aluminum capacitors (1000  $\mu$ F, 50 Vdc) were used as storage capacitor CST. It should be noted that the buck converter shares the output filter, i.e., output inductor LF and output capacitor CF, with the full-bridge converter. The switching frequency of the buck converter was set to approximately 100 kHz, i.e., close enough to the 110-kHz frequency of the full-bridge converter to keep the output filter inductor current virtually unchanged

Fig. 7. Control implementation of the proposed method in PFC applications. capacitor needs to store significant energy, for example, in PFC applications, additional energy-storage capacitor CST may not be needed.



When the proposed efficiency optimization method is applied to the ac–dc PFC front-end, it is necessary to recognize that the line current harmonic limit specifications need to be met down to 75 W of input power [12]. As a result, a straightforward implementation of this method, where the front-end power converter is periodically turned on and off with an arbitrary frequency, is possible only below the input power of 75 W. Because of the required compliance with the line current harmonic limit specifications at input power levels above 75 W, the turning off and on of the converter can only be done within half-line cycles, as illustrated in Fig. 7. In the control approach shown in Fig. 7, the PFC converter is kept OFF near the zero crossings of the line current, and is enabled for power processing around the peaks of the line current. Since this conduction-angle control generates line current distortions that increase as turn OFF time  $T_{OFF}$  increases, the maximum duration of OFF-time  $T_{OFF}$  is limited by the required harmonic-limit compliance of the line current. This maximum OFF-time can be easily figured out for a given power level either by using simulation or calculation software.

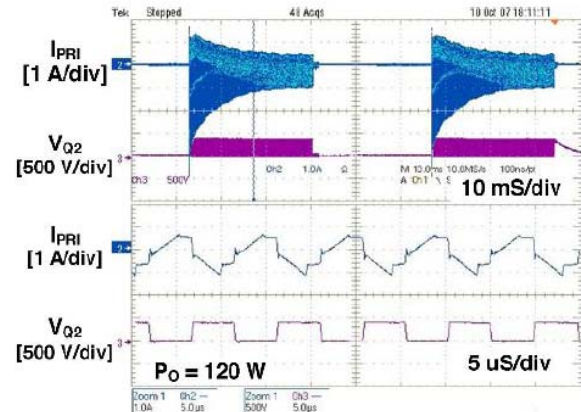
#### V. EXPERIMENTAL RESULTS

The performance of the proposed technique was separately evaluated on a 500-W dc–dc converter and a 1-kW ac–dc PFC boost frontend rectifier. The circuit diagram of the 500-W dc–dc converter prototype is

shown in Fig. 8. The circuit in Fig. 8 implements the proposed method of light-load efficiency optimization according to Fig. 6(a), where  $V_1 = V_2$  and  $L_1$  is the leakage inductance of transformer TR, i.e., it combines a zero-voltage-switching (ZVS) full-bridge converter with phase-shift control with a synchronous buck converter discharging circuit. The 500-W dc-dc prototype was designed to operate from a 400-V dc input and deliver up to 42 A at a 12-V output.

The full-bridge converter operating at 110-kHz switching frequency was implemented with an IRFP23N50L MOSFET from IR for each bridge switch Q1–Q4, whereas a FDB045AN08 MOSFET from Fairchild was employed for each synchronous rectifier SR1 and SR2. Transformer TR was built using a pair of ferrite E-cores (E34/26/9-H7C4) with 44 turns of magnet wire (AWG #18) for the primary winding and 2 turns of copper foil (10 mil, 20 mm) for each of the secondary windings. Output filter inductor  $L_F$  was built using a toroidal high-flux core (58894A2,  $\mu = 60$ ) from Magnetics with eight turns of magnet wire (six strands, AWG #18). Four low-voltage aluminum capacitors (1000  $\mu$ F, 16 Vdc) were used for output capacitor CF. The buck converter that is periodically turned on at light loads to deliver power from energy-storage capacitor CST was implemented with an FDP047AN08 MOSFET from Fairchild for both the buck switch S1 and synchronous rectifier switch S2. Schottky diodes MBR1080G from On Semi were used for charging diodes D1 and D2. Finally, six low-voltage aluminum capacitors (1000  $\mu$ F, 50 Vdc) were used as storage capacitor CST. It should be noted that the buck converter shares the output filter, i.e., output inductor  $L_F$  and output capacitor CF, with the full-bridge converter. The switching frequency of the buck converter was set to approximately 100 kHz, i.e., close enough to the 110-kHz frequency of the full-bridge converter to keep the output filter inductor current virtually unchanged during transitions between the full-bridge and buck operation, thus ensuring smooth transitions between these two modes of operation. In fact, no significant variations of the output voltage during the mode transitions were observed in the experimental prototype converter. Since the full-bridge converter and the buck converter do not operate at the same time, a frequency synchronization of two converters was not necessary. The maximum output power of the buck converter was designed to be approximately 140 W, which is enough to deliver up to 25% of the total output power. Fig. 9 shows the measured waveforms of the prototype circuit at approximately 120 W. Time periods  $T_{ON}$  and  $T_{OFF}$  are approximately 27 and 26 ms, respectively. In order to reduce the voltage ripple of storage capacitor CST and operate below audible frequency, the frequency at which

the power converter is turned on and off is set to be approximately 19 Hz.



As observed from Fig. 9, duty cycle  $D$  of the prototype circuit at 120 W is approximately 50%, which is slightly higher than the optimum duty cycle at this output power. Fig. 10 shows measured efficiency of the proposed converter along with the measured efficiencies of the full-bridge converter and the buck converter. As can be seen from Fig. 10, the proposed Fig. 11. Circuit diagram of the experimental 1-kW PFC boost rectifier converter exhibits higher efficiencies below approximately 100 W. The improvement of the efficiency is more pronounced as the load becomes lighter. For example, at 50 W, which is 10% of the full load, the efficiency improvement is around 8%, whereas at 25 W, i.e., at 5% of the full load, the improvement is approximately 24%. It should be noted that the power consumption of the controller and gate drive circuit, which is approximately 1 W, is not included in the measured results shown in Fig. 10.

Fig. 9. Measured primary current  $I_{PR1}$  and switch Q2 drain-to-source voltage  $V_{Q2}$  waveforms of ZVS full-bridge converter prototype. Time scale for upper two traces is 10 ms/div. Time scale for bottom two traces is 5  $\mu$ s/div.

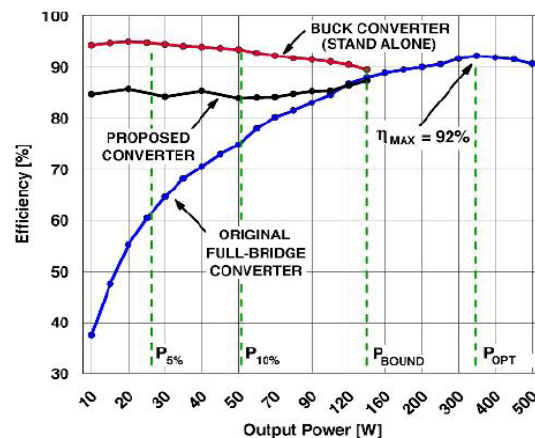


Fig. 10. Measured efficiencies of the original full-bridge converter, the stand-alone buck converter, and the proposed converter as functions of output power.

This power loss is excluded since no effort was made to optimize the controller and gate drive circuit used in the prototype. As shown in Fig. 10, the original full-bridge converter exhibits a low efficiency at light loads because soft switching is lost at light loads. Generally, the light-load efficiency could be improved by employing switching devices that have lower output capacitances. However, since these devices typically have higher turn-ON resistances, the full-load efficiency is significantly degraded by this design choice. The proposed approach offers improvements of light-load efficiency without adversely affecting the full-load efficiency since it allows the use of optimal switching devices.

Fig. 11 shows the circuit diagram of the PFC boost rectifier prototype, which is built to evaluate the performance of the proposed method in ac-dc applications. The 1-kW, 110-kHz PFC boost rectifier prototype was designed to operate from a universal ac-line input (90–264 V<sub>rms</sub>) and deliver up to 2.5 A from a 400-V output. The prototype employs two IPP60R099CS MOSFETs ( $V_{DS} = 600$  V,  $R_{DS} = 0.099$   $\Omega$ ) in parallel for boost switch *S* and a CSD10060 SiC diode ( $V_{RRM} = 600$  V,  $I_{FAVM} = 10$  A) for boost diode *D*. In this implementation, 560- $\mu$ F bulk capacitor *CB* that is sized based on the hold-up-time requirement also serves as energy-storage capacitor *CST*. Fig. 12 shows the oscillograms of the input current, input voltage, and output voltage waveforms of the PFC rectifier prototype with the conduction-angle control. To simplify the experiment, i.e., to avoid implementing a conduction-angle control itself, the conduction angle of the input voltage waveform was actually controlled by a programmable ac source (6000LX, California Instrument). Because in the PFC boost rectifier, the input current waveform follows the input voltage waveform, the desired operation was achieved without any modifications of the PFC control circuit. The measured efficiencies of the PFC rectifier with and without conduction-angle control are shown in Fig. 13. As can be seen from Fig. 13, conduction-angle control was applied at power levels below 100 W, i.e., below 10% of the full power. With the conduction-angle control, the prototype PFC rectifier exhibits higher light-load efficiencies. In fact, at the same power level, the efficiency gains are larger as conduction time  $T_{ON}$  decreases from 7 to 1 ms. However, as the conduction time reduces, the maximum power that can be delivered to the output also reduces. The maximum light-load efficiency gains can be obtained by implementing active conduction time control, i.e., by reducing conduction time  $T_{ON}$  as the output power reduces. With this kind of control, the light-load efficiency is represented by the dashed line in Fig. 13.

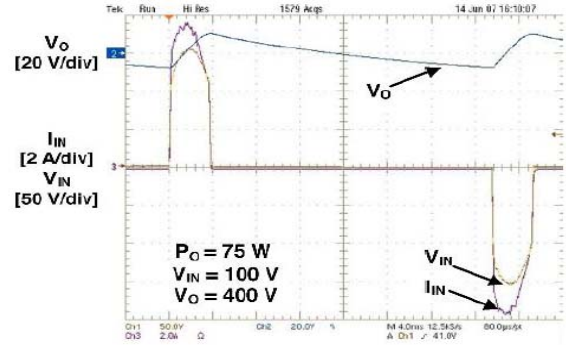


Fig. 12. Measured waveforms of the experimental PFC boost rectifier.  $V_{IN}$  is line voltage,  $I_{IN}$  is line current, and  $V_O$  is output voltage.

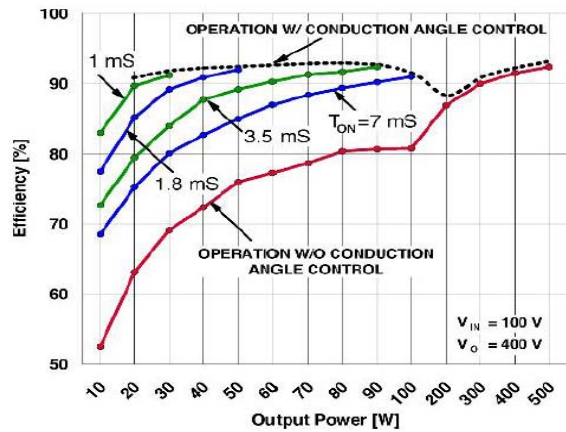


Fig. 13. Measured efficiency of the PFC rectifier as functions of output power for different conduction times  $T_{ON}$ . The dashed line represents efficiency that can be obtained by changing (decreasing)  $T_{ON}$  as output power decreases.

## VI. SUMMARY

A method of improving the light-load efficiency of power converters has been proposed in this paper. In the proposed method, the light-load efficiency improvement is achieved by periodically turning off the power converter to reduce switching-related losses. During the time periods the converter is turned off, the required load power is supplied from an energy-storage device. During the time periods when the converter is delivering power to the load and charging the energy-storage device, it is controlled so that it operates at a power level that corresponds to the maximum conversion efficiency.

The proposed efficiency optimization method is applicable to any power-conversion dc-dc or ac-dc system or topology. Generally, the energy-storage medium can be any component/device that can store energy, for example, capacitors, batteries, flywheels, etc.

The performance of the proposed method was verified on two experimental prototypes: a 500-W ZVS full-bridge dc-dc converter and a 1-kW boost PFC converter. Both prototypes showed remarkable

light-load efficiency improvements with the proposed approach all the way down to 5% load.

## REFERENCES

- [1] Power Integrations, Inc. Green Room page [Online]. Available: <http://www.powerint.com/greenroom/index.html>
- [2] 80Plus Program [Online]. Available: <http://www.80plus.org/index.htm>
- [3] Climate Savers Computing Initiative (CSCI) Web Site [Online]. Available: <http://www.climatesaverscomputing.org/>
- [4] Climate Savers Computing Initiative (CSCI) Web Site, Efficiency Specification page [Online]. Available: <http://www.climatesaverscomputing.org/about/faq/#4>
- [5] Environmental Protection Agency (EPA) Energy Star Program, Version 5.0 Computer Specifications [Online]. Available: [http://www.energystar.gov/index.cfm?c=revisions.computer\\_spec](http://www.energystar.gov/index.cfm?c=revisions.computer_spec)
- [6] F. C. Lee, P. Barbosa, P. Xu, J. Zhang, B. Yang, and F. Canales, "Topologies and design considerations for distributed power system applications," *Proc. IEEE*, vol. 89, no. 6, pp. 939–950, Jun. 2001.
- [7] F. C. Lee, M. Xu, S. Wang, and B. Lu, "Design challenges for distributed power systems," in *Proc. IEEE Int. Power Electron. Motion Control Conf. (IPEMC)*, Shanghai, China, 2006, pp. 1–15 (Key note speech PA1).
- [8] H. S. Choi and D. Y. Huh, "Techniques to minimize power consumption of SMPS in standby mode," in *IEEE Power Electron. Spec. Conf. (PESC) Rec.*, 2005, pp. 2817–2822.
- [9] P. Vinciarelli, "Adaptive boost switching preregulator and method," U.S. Patent 5 289 361, Feb. 22, 1994.
- [10] S. W. Hobrecht and R. G. Flatness, "Multiple phase switching regulators with stage shedding," U.S. Patent 6 674 274, Jan. 6, 2004.
- [11] J. Choi, D. Huh, and Y. Kim, "The improved burst mode in the stand-by operation of power supply," in *Proc. IEEE Appl. Power Electron. Conf. (APEC) 2004*, pp. 426–432.
- [12] Electromagnetic Compatibility (EMC)—Part3: Limits—Section 2: Limits for Harmonic Current Emissions (Equipment Input Current < 16 A Per Phase), IEC Standard 61000-3-2, 1998.